JACS
JOURNAL OF THE AMERICAN CHEMICAL SOCIETY

Article

pubs.acs.org/JACS

A Trialkylphosphine-Driven Chemical Transformation Route to Ag- and Bi-Based Chalcogenides

Shi-Kui Han,[†,§] Chao Gu,[†,§] Ming Gong,[‡] and Shu-Hong Yu*[,†]

[†]Division of Nanomaterials and Chemistry, Hefei National Laboratory for Physical Sciences at Microscale, Collaborative Innovation Center of Suzhou Nano Science and Technology, Department of Chemistry, University of Science and Technology of China, Hefei, Anhui 230026, P. R. China

[‡]Lab of Mechanical and Material Science, School of Engineering Science, University of Science and Technology of China, Hefei, Anhui 230026, P. R. China

Supporting Information

ABSTRACT: From the standpoint of chemistry, the metastable nature of nanocrystals provides us plentiful ground for the research of new nanoscale structural transformations. Herein, we report a new phenomenon that trialkylphosphine (TAP) can extract the Ag^+ and Bi^{3+} from their nanostructural chalcogenides and reduce them to the zerovalent state. Based on this principle, a trialkylphosphine-driven chemical transformation route has been developed for the synthesis of a series of metals and metal-sulfide heterostructures with multiple sulfides as the precursors. Using this reaction principle, Ag, Bi, Ag-Ni_3S_2, Ag-ZnS, Ag-$AgInS_2$, Ag-Bi, and Bi-Cu_7S_4 nanostructures can be successively synthesized. These Ag- or Bi-based metal chalcogenide heteronanostructures with interesting optical properties or multifunctionalities could be of special interest for a variety of applications, including high-performance catalysis, biological and biomedical sensing, photovoltaic devices, and a new generation of optoelectronic devices.

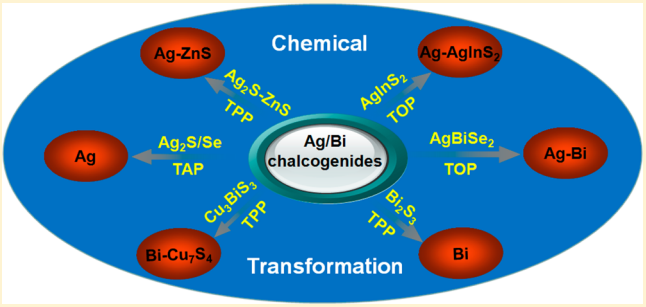

INTRODUCTION

During the last couple of decades there has been increasing interest in nanoscale objects owing to their unique physical and chemical properties compared with corresponding bulk materials.[1−4] However, as a new branch of synthetic chemistry, colloidal synthesis of nanostructures is difficult to control for its too much depending on the rates of nucleation and growth of nanoparticles.[5−14] Development of synthetic approaches to produce a new class of nanocrystals with uniform size, shape, chemical composition, and morphology is extremely important for further fundamental studies and practical applications.[15−23] To date, there are four types of solution routes in the literature[24] for transforming one crystalline nanomaterial into another desired crystalline nanomaterial, i.e., the ion exchange reaction,[25−34] the Kikendall effect,[35−38] stabilizer-depleted binary semiconductor nanocrystals,[24,39−41] and thermally induced phase segregation and solid-state diffusion.[17,42−44] Ion exchange involves replacing the ion in an ionic nanocrystal lattice with a different ion. Utilizing the cation exchange reaction, Alivisatos and co-workers successfully synthesized CdS-Ag_2S superlattices,[32] CdS-Cu_2S heterostructures,[34] and III−V (GaAs, InAs, GaP, and InP) nanocrystals.[45] Moreover, Teranishi and co-workers[29] prepared CdS/CdTe heterodimers through an anion exchange reaction of ionic CdS nanoparticles with tri-n-octylphosphine telluride. In Kikendall effect, hollow nanocrystals can be synthesized because of the difference in diffusion rates between two components in a diffusion couple, including the reaction of metal nanocrystals to a binary compound or converting one binary compound into another binary/ternary metal (mixed) oxide or sulfide.[35] The stabilizer-depleted binary semiconductor nanocrystals method can transform binary materials into unary semiconductors because of a manifold of long and short range interparticle forces brought about by partial removal of the stabilizer shell. Adopting this method, Kotov and co-workers have successfully converted CdSe/CdTe nanoparticles into unary Se/Te nanowires and branched Te nanocrystals.[40,41] In addition, Zhang and co-workers transformed the binary Sb_2Te_3 nanoplates into unary 3D porous Te plates.[24] As for the thermally induced phase segregation and solid-state diffusion method, it can transform one kind of heteronanostructure or unary semiconductors into another kind of heteronanostructure. Banin and co-workers[43] found that Au/InAs core/shell nanocrystals can be oxidized into Au/In_2O_3 core/shell nanocrystals under air by solid-state diffusion. Similarly, we reported a facile one-pot method to prepare colloidal $AgFeS_2$ nanocrystals.[44] Such ternary $AgFeS_2$ nanocrystals are not stable and will transform into Ag_2S−Fe_7S_8 heteronanostructures by thermally induced phase segregation and solid-state diffusion at higher temperature.

Received: January 3, 2015
Published: April 10, 2015

DOI: 10.1021/jacs.5b00041
J. Am. Chem. Soc. 2015, 137, 5390−5396

Trialkylphosphine (TAP), regarded as a nanocrystal surface stabilizer, a phosphorus source in chemical reaction, or a chemical reagent in the formation of TAP-X (X = S, Se, Te) complexes, has been extensively used in colloidal synthesis of nanostructures.[37] Schaak and co-workers[46] found that tylphosphine (TOP) can extract selenium or sulfur from selenium- or sulfur-rich metal chalcogenides and transform them into lower-chalcogen compounds. While in the reverse cation exchange reaction, tributylphosphine (TBP),[28] as a soft base, can bind strongly to Ag^+ cations in the precursor lattice and form intermediate complexes to promote the cations exchange in solution within the anion sublattice.

Herein, we report a new strategy that TAP can extract the Ag^+ and Bi^{3+} from their nanostructural chalcogenides (except telluride) and reduce them to the zerovalent state. Using this reaction principle, Ag, Ag-Ni_3S_2, Ag-ZnS, Ag-$AgInS_2$, Ag-Bi, Bi, and Bi-Cu_7S_4 nanostructures can be successively synthesized, as illustrated schematically in Scheme 1. Thus, it is expected that this trialkylphosphine-driven chemical transformation route can be a powerful supplement to the synthesis pathways mentioned above, facilitating composition and phase tunable fabrication of metals and metal-sulfide heterostructure systems.

Scheme 1. Synthetic Routes for the Chemical Transformation of Ag- and Bi-Based Chalcogenides

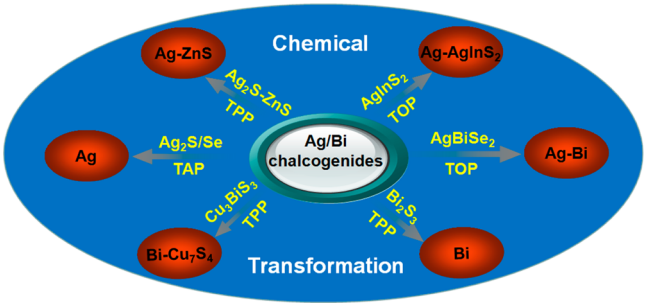

RESULTS AND DISCUSSION

First of all, the Ag_2S nanocrystals were synthesized by using the reported solution method.[47] Figure 1a shows a typical transmission electron microscopy (TEM) image of the colloidal Ag_2S nanocrystals with a diameter of about 10 nm. The typical powder X-ray diffraction (XRD) pattern displayed in Figure 1b identifies these colloidal nanocrystals as a crystalline phase of Ag_2S (JCPDS no. 14-0072, monoclinic, a = 4.226 Å, b = 6.928 Å, c = 7.858 Å). Chemical transformation reactions were performed by adding 0.1 g triphenylphosphine (TPP) into Ag_2S solutions in oleylamine at 220 °C under N_2. The powder XRD was carried out on the as-transformed products, as shown in Figure 1b. All of the peaks in the XRD pattern matched those of cubic Ag, and the calculated lattice constants were a = 4.085 Å (JCPDS no. 89-3722). Figure 1c shows a typical TEM image of the as-transformed products. It is obvious that the products are monodispersed nanoparticles with an average size of about 15 nm. The structural analysis from a high-resolution TEM (HRTEM) image further shows that the Ag nanoparticles are of high crystallinity, and the interplanar distances of 2.37 Å are clearly observed, corresponding to the (111) plane of cubic Ag (Figure 1d). Likewise, using TOP or TBP instead of TPP, Ag_2S nanocrystals can also be transformed into Ag confirmed by XRD patterns (see Supporting Information Figure S1).

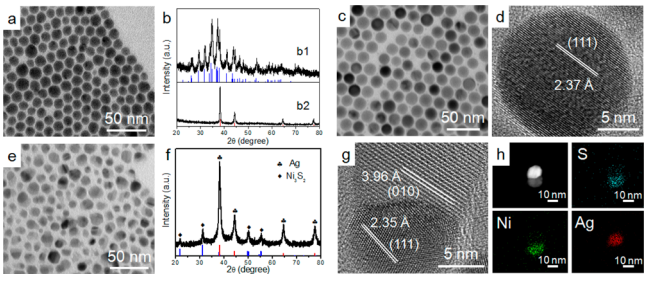

Figure 1. (a) TEM image of the Ag_2S nanocrystals. (b) XRD patterns of the Ag_2S nanocrystals (b1) before chemical transformation and (b2) after chemical transformation. (c) TEM and (d) HRTEM image of the Ag nanocrystals. (e) TEM image, (f) XRD, (g) HRTEM images and (h) STEM-EDS elemental mapping images of the Ag-Ni_3S_2 heteronanostructures.

Under the same conditions, if we treat the Ag_2Se (JCPDS no. 24-1041) nanocrystals[48] with TPP, it is clear that the chemical transformation reaction will not occur (Figure S1), while TOP can transform Ag_2Se nanocrystals into Ag (Figure S1). This is due to the more "positive" phosphorus atom linked with three electron-donating alkyl groups in TOP, causing its stronger reducibility toward Ag^+ in Ag_2Se. Furthermore, as a common sense, element selenium can easily dissolve into TOP but not TPP, which results from the large formation constant of TOP-Se complexes. So the high reactivity between TOP and Se also contributes to the transformation. As shown in Figure S1, for the Ag_2Te (JCPDS no. 34-0142) nanocrystals, neither TPP nor TOP can induce the chemical transformation reaction to proceed. Similar to the above, the poor reducibility of trialkylphosphine is unable to reducing Ag^+ because of the high binding energy in Ag_2Te. Moreover, element Tellurium dissolves into TOP very slowly, which indicates the reactivity between TOP and Te is rather low.

After the chemical transformation reaction, a question came: where the element S went ? Did it still stayed in the solution as the TAP-S complexes or came out in other forms, such as H_2S, or SO_2 ? So in-depth study was needed. Further experiment was done by adding some acetylacetone nickel to the Ag_2S solution at the beginning of the transformation reaction (see Experimental Section). The corresponding TEM image (Figure 1e) indicates that the products are monodispersed nanoparticles. Based on the XRD pattern (Figure 1f), it is obvious that the obtained products are composed of crystalline phases of cubic Ag (JCPDS no. 89−3722) and hexagonal Ni_3S_2 (JCPDS no. 44−1418, a = 5.745 Å, c = 7.135 Å). Further characterization by HRTEM image (Figure 1g) indicates that the nanoparticles are composed of high crystalline Ag and Ni_3S_2, and the lattice distances are measured to be 2.35 and 3.96 Å, corresponding to those of (111) plane of cubic Ag and (010) plane of hexagonal Ni_3S_2, respectively. Figure 1h shows the high-angle annular dark field scanning TEM (HAADF-STEM) image of the prepared heteronanostructures. The clear contrast between the two segments indicates that the heteronanostructure consists of two different components. Moreover, the elemental distributions of Ag and Ni in the two-component heteronanostructures (Figure 1h) were obtained by STEM-EDS elemental mapping. The green regions in the image are the Ni-containing component, and the red are the Ag-containing component, which further demonstrates the formation of the heteronanostructures. Thus, all the results and

DOI: 10.1021/jacs.5b00041
J. Am. Chem. Soc. 2015, 137, 5390−5396

characterizations show that element S indeed exists in the solution.

According to this principle, the Ag chalcogenides-based heterostructures can be transformed into Ag-based heterostructures. Then, match-like Ag_2S-ZnS heteronanostructures were prepared as adapted from previously reported methods.[49] The TEM, XRD (Figure 2a,b), and STEM-EDS elemental

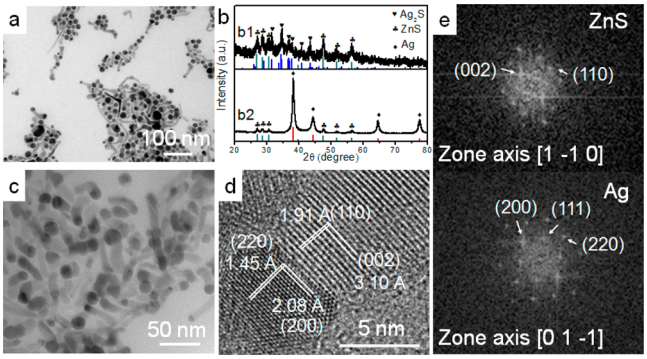

Figure 2. (a) TEM image of the Ag_2S-ZnS heteronanostructures. (b) XRD patterns of the Ag_2S-ZnS heteronanostructures (b1) before chemical transformation and (b2) after chemical transformation. (c) TEM and (d) HRTEM image of the Ag-ZnS heteronanostructures. (e) FFT patterns of the HRTEM images of the segments of ZnS and Ag.

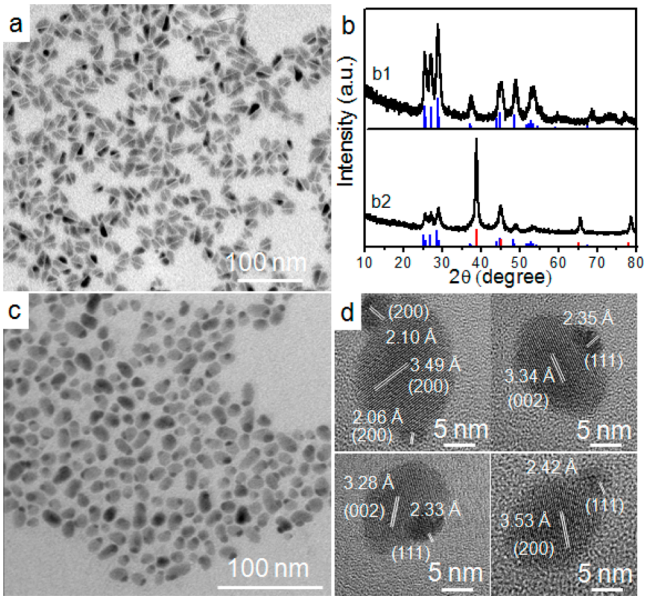

Figure 3. (a) TEM image of $AgInS_2$ nanocrystals. (b) XRD patterns of $AgInS_2$ nanocrystals (b1) before chemical transformation, and (b2) after chemical transformation. (c) TEM and (d) HRTEM image of the Ag-$AgInS_2$ heteronanostructures.

mapping (Figure S2) results confirmed that the heteronanostructures were successfully synthesized. After the similar chemical transformation reaction, the domains of Ag_2S were also transformed into Ag. As shown in Figure 2b, the XRD result clearly shows that the typical diffraction peaks of the Ag_2S disappear, and the new diffraction peaks of Ag appear instead. The corresponding TEM image in Figure 2c indicates that the morphology of the products does not change and preserves its match-like shape. The HRTEM and fast Fourier transform (FFT) images (Figure 2d,e) further confirm the orientational relationship between Ag and ZnS. A straightforward relationship of plane epitaxy can be proposed for the (002) planes (d = 3.10 Å) of ZnS (JCPDS no. 36-1450) and the (200) planes (d = 2.04 Å) of Ag. The large lattice mismatch between (110) ZnS and (220) Ag are $[(1.91 - 1.45)/1.91 \times 100\%] = 24\%$ which may cause the local curving near interface junction or a decrease in the total surface energy to accommodate it.[49] The STEM-EDS elemental mapping results (Figure S3) demonstrate that the segments of the match heads are Ag, while the match sticks are ZnS.

As such, this approach can also be expanded to transforming ternary Ag chalcogenides to Ag-based heterostructures. Ternary $AgInS_2$ was prepared by the reported solution method.[50] The TEM and XRD (Figure 3a, b1) results confirmed that the ternary $AgInS_2$ (JCPDS no. 25-1328) nanocrystals were successfully synthesized. Then, chemical transformation reactions were performed by adding 0.2 mL TOP into $AgInS_2$ solution in oleylamine at 250 °C for 1 h under N_2. The powder XRD was carried out on the as-obtained products, as shown in Figure 3b. The typical diffraction peaks of the ternary $AgInS_2$ nanocrystals weakened and the cubic Ag diffraction peaks (JCPDS no. 89-3722) appeared in the XRD pattern (Figure 3b). So the obtained products are heterostructures composed of crystalline phases of cubic Ag and $AgInS_2$ based on the XRD pattern (Figure 3b) and TEM image (Figure 3c). The HRTEM images (Figure 3d) further confirm the orientational relationship between Ag and $AgInS_2$. The structural analysis from the HRTEM images (Figure 3d) reveals that the element Ag could be extracted from both ends, one end, and the middle of the $AgInS_2$ nanocrystals. Furthermore, when 1 mL TOP was added into $AgInS_2$ solution and reacted for 10 h, the $AgInS_2$ nanocrystals would be completely transformed into Ag nanocrystals finally (see Figure S4). Why is there no byproduct of In_2S_3 existence in the final solution? It is probably because of element indium and sulfur existing in the solution formed $In_2S_4^{2-}$ ions as the surfactant, which have been reported by Talapin et al.[11]

Ternary nanocrystals of $AgFeS_2$ (JCPDS no. 65-2736) and $AgBiSe_2$ (JCPDS no. 74-0842) using the similar methods[44,S1] were also treated under the same conditions. For the $AgFeS_2$ nanocrystals, they also transformed into Ag nanocrystals finally, as shown in Figure S5. While for $AgBiSe_2$ nanocrystals (Figure S6a), the pure Ag nanocrystals have not been obtained. Based on the analysis of the XRD pattern (Figure 4a) and TEM images (Figures 4b and S6b), the final products are the Ag-Bi core−shell nanocrystals. The analysis of the lattice spacing from the HRTEM image (Figure 4c) reveals that the (111) planes of Ag are coincident with the (012) planes of Bi (JCPDS no. 44-1246). The image obtained by line-scan energy-dispersive X-ray spectroscopy (Figure 4d) further clearly revealed that the nanoparticles were core−shell nanostructures consisting of an Ag core and a Bi shell.

Based on the above experimental results, it can be seen that Bi^{3+} can also be extracted from the ternary $AgBiSe_2$ nanocrystals. And another question comes whether Bi^{3+} can be extracted from all the Bi-based chalcogenides. So Bi_2S_3 nanorods[S2] were synthesized and treated using similar chemical transformation reaction. From the TEM image (Figure 5a) and XRD pattern (Figure S7a), it is obvious that the Bi_2S_3 nanorods were successfully synthesized. For the chemical transformation process, time-dependent experiments were conducted, as shown in Figure 5b−f. At the early stage of the chemical transformation process, the domain of Bi appeared on the tips

DOI: 10.1021/jacs.5b00041
J. Am. Chem. Soc. 2015, 137, 5390−5396

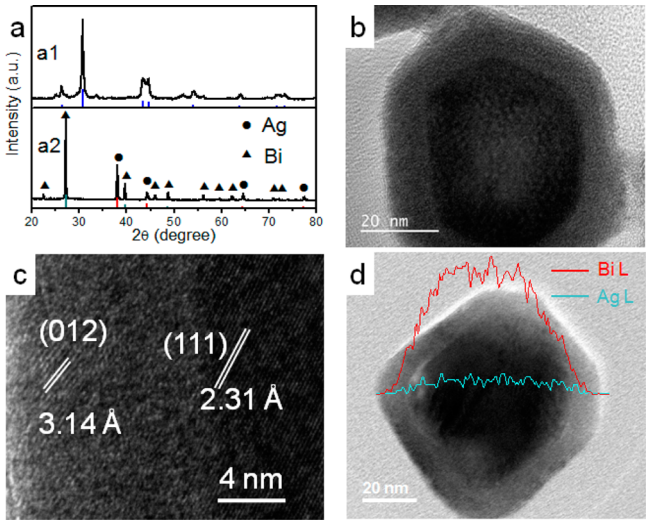

Figure 4. (a) XRD patterns of the $AgBiSe_2$ nanocrystals (a1) before chemical transformation, and (a2) after chemical transformation. (b) TEM image, (c) HRTEM image and (d) EDS line scan profiles of the Ag-Bi core−shell heteronanostructures.

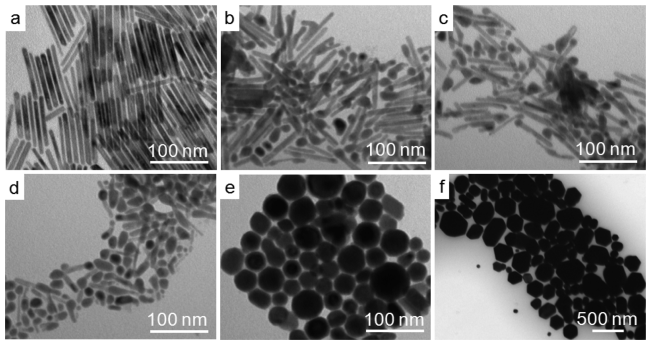

Figure 5. TEM images of the Bi_2S_3 nanocrystals and their corresponding products after chemical transformation reactions for different time: (a) Bi_2S_3 and (b) 5, (c) 10, (d) 20, (e) 30, and (f) 60 min.

of the Bi_2S_3 nanorods. And then the segment of Bi grew up as the reaction progressed. Finally, the Bi_2S_3 nanorods disappeared and completely transformed into Bi (JCPDS no. 44-1246) nanocrystals, which was confirmed by the XRD result (Figure S7b). To expand this reaction, Cu_3BiS_3 nanocrystals (JCPDS no. 71-2115)[53] were successfully prepared using the reported solution method (Figure S8a, b1). The same as the transformation process of Bi_2S_3 nanorods, the domain of Bi also appeared first on the edge of the Cu_3BiS_3 nanocrystals (Figure S8c). As the reaction progressed, the segment of Bi grew up and Cu_3BiS_3 nanocrystals finally transformed into mushroom-shaped Bi-Cu_7S_4 heteronanostructures, which are based on the analysis of XRD pattern (Figure S8b) and TEM image (Figure S8d, 6a).

Compared with $AgInS_2$, after extraction of Bi, Cu_7S_4 nanostructures are also formed in the final solution. This is because the binding energy of Cu_7S_4 is very strong in this situation that is inclined to form this kind of nanostructures. The characterization by the corresponding HRTEM image (Figure 6b) further indicates that the mushroom-shaped nanocrystals are of high crystallinity. The fringe spacing of the mushroom stalk is clearly discerned to be 2.61 Å, corresponding to the (20 0 1) planes of monoclinic Cu_7S_4

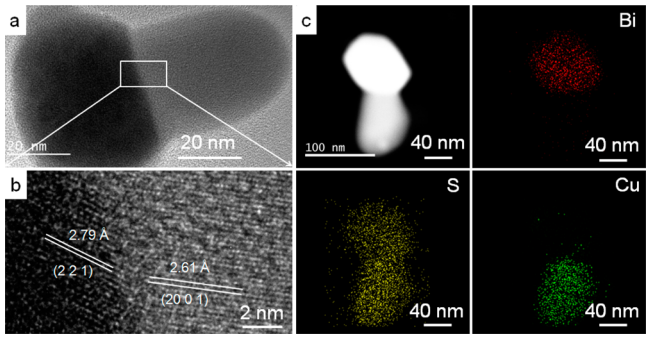

Figure 6. (a) TEM image, (b) HRTEM image, and (c) STEM-EDS elemental mapping images of the products obtained by chemical transformation of Cu_3BiS_3 nanocrystals.

(JCPDS no. 23-0958). While the fringe spacing of the mushroom head measured to be 2.79 Å, which cannot be matched with any plane of hexagonal Bi (JCPDS no. 44-1246). Moreover, the elemental distributions of Bi, Cu, and S in the two-component heteronanostructures were obtained by STEM-EDS elemental mapping, as shown in Figure 6c. It is surprising that the element S exists in both components of the heteronanostructures. That is, the obtained heteronanostructures are not Bi-Cu_7S_4 but Bi_2S_3-Cu_7S_4. But from the analysis of XRD pattern, there is no existence of the phase of Bi_2S_3. Besides, from the above results, it is very clear that the Bi_2S_3 has been completely transformed into Bi in the existence of TPP at the temperature of 220 °C. We proposed that the transformed products of Cu_3BiS_3 nanocrystals are Bi-Cu_7S_4 heteronanostructures. Bi nanocrystals with low melting point are widely used for nanowire growth via the solution-liquid−solid strategy as a catalyst.[54] With this unique property, Bi nanocrystals are very active under the radiation of the high-energy electron beam. Thus, Bi will react with the sulfur diffusing from the segment of monoclinic Cu_7S_4 to form Bi_2S_3-Cu_7S_4 heteronanostructures. That is why we cannot observe the Bi-Cu_7S_4 heteronanostructures by the analysis of HRTEM and STEM-EDS elemental mapping. So the fringe spacing of the mushroom head measured to be 2.79 Å should correspond to the (2 2 1) planes of orthorhombic Bi_2S_3 (JCPDS no. 65-2435).

Previous studies have shown that TOP can transform the selenium- or sulfur-rich metal chalcogenides into lower chalcogen compounds through extraction of selenium or sulfur, such as $SnSe_2$, $CoSe_2$, and $NiSe_2$, which convert to SnSe, Co_9Se_8, and Ni_3Se_2, respectively.[46] While Alivisatos and co-workers[28] reported that TBP, as a soft base, could bind strongly to Ag^+ cations in the precursor lattice and form intermediate complexes to promote the reverse cations exchange in solution under ambient conditions. In our experiments, we found that not only Ag-TAP intermediate complexes but also S/Se-TAP were formed, which will assist the chemical transformation process. Taking the chemical transformation process of Ag_2S nanocrystals as an example, there is a chemical equilibrium between Ag_2S and Ag^+ and S^{2-} in oleylamine solution. TAP, as a soft base, bound strongly to Ag^+ cations first in reaction solution. And then Ag^+ cations were reduced to Ag by TAP serving as the reducing agent at high temperatures. This would break the solubility equilibrium of Ag_2S in the solution and promote the chemical transformation of Ag_2S nanocrystals into Ag nanostructures. However, as for Ag_2Se nanocrystals, TPP cannot transform them to Ag nanocrystals while TOP can, which means that the binding between Ag^+ and TAP is not

DOI: 10.1021/jacs.5b00041
J. Am. Chem. Soc. 2015, 137, 5390−5396

enough to transform Ag_2Se into Ag. As we mentioned above, forming S/Se-TAP complexes also contributes to this transformation process. When it comes to the Ag_2Te nanocrystals, neither TPP nor TOP can transform them to Ag nanocrystals, which indicates that the binding energy between Ag^+ and Te^{2-} is stronger than Ag-TAP and Te-TAP. Therefore, the binding energies between Ag/Bi and S/Se/Te, Ag/Bi and TAP, and S/Se/Te and TAP are crucial to the transformation process. Besides, it is similar for the $AgInS_2$ and Cu_3BiS_3. When extracting Ag from $AgInS_2$, the binding energy of $In_2S_4^{2-}$ is strong enough to maintain stable in the solution. While for the Cu_3BiS_3, the binding energy of Cu_7S_4 is very strong in this situation that is inclined to recrystallize to form nanocrystals. Based on the above experimental results and analysis, it is obvious that TAP can reduce Ag- and Bi-based chalcogenides (except telluride) to the zerovalent state. For high-valence metal chalcogenides (e.g., $SnSe_2$, $CoSe_2$, and $NiSe_2$), TAP can just reduce them to low-valence chalcogenides (e.g., SnSe, Co_9Se_8, and Ni_3Se_2). While for Zn- and Cd-based chalcogenides, according to the above experimental results, ZnS segments will not change after the chemical transformation of Ag_2S-ZnS to Ag-ZnS heteronanostructures. What's more, plenty of work has reported that TOP is usually used to synthesize Cd-based chalcogenides nanocrystals as the capping agents,[12,55,56] especially in the quantum dots synthesis. Therefore, there is enough evidence showing that TAP has no effect on Zn- and Cd-based chalcogenides.

CONCLUSIONS

In summary, we have developed a trialkylphosphine-driven chemical transformation route for the synthesis of metal and metal sulfide heterostructures with multiple sulfides as the precursors. The results demonstrated that trialkylphosphine can extract the Ag^+ and Bi^{3+} from their nanostructural chalcogenides and reduce them to the zerovalent state in solution reaction. This general chemical transformation strategy has three important implications. First, it represents a green and economical synthesis strategy because noble metal Ag can be recycled through solution process as Ag_2S and Ag_2Se can be reduced to Ag completely. Second, it is an addition to the growing toolbox of fabricating Ag-metal chalcogenides heteronanostructures which are significant in photocatalytic and photothermal areas. Ag-Ni_3S_2, Ag-ZnS, and Ag-$AgInS_2$ heteronanostructures with well-defined morphology can be synthesized using this method. Third, it provides a new avenue for the synthesis of composition and shape controllable Bi and Bi-based nanostructures. For example, Bi-Bi_2S_3 nanorods, Ag-Bi core−shell nanostructures, and Bi-Cu_7S_4 mushroom heteronanostructures can be obtained by this approach. Such a colloidal chemical transformation method provides a new strategy for controlled synthesis of a family of Ag- or Bi-based metal chalcogenide heteronanostructures, which may have interesting optical properties or multifunctionalities for applications in various fields.

EXPERIMENTAL SECTION

Chemicals. The chemicals sodium diethyldithiocarbamate ($Na(S_2CNEt_2)$), $Fe(NO_3)_3{\cdot}9H_2O$, $Bi(NO_3)_3{\cdot}5H_2O$, $AgNO_3$, $ZnCl_2$, $BiCl_3$, $InCl_3$, sulfur powder, selenium powder, tellurium powder, oleic acid (OA), 1-dodecanethiol (DDT), triphenylphosphine (TPP), and tributylphosphine (TBP) were purchased from the Shanghai Reagent Company (P. R. China). Octadecylamine (ODA, 90%) and oleylamine (OLA, 70%) were purchased from Aldrich. 1-Octadecene (ODE, 90%), tri-*n*-octylphosphine (TOP, 90%), acetylacetone copper ($Cu(acac)_2$), and acetylacetone nickel ($Ni(acac)_2$) were purchased from Alfa Aesar. All chemicals were used as received without any further purification.

Synthesis of $Ag(S_2CNEt_2)$, $Zn(S_2CNEt_2)_2$, $In(S_2CNEt_2)_3$, and $Fe(S_2CNEt_2)_3$ Precursors. In a typical reaction for $Ag(S_2CNEt_2)$, $Na(S_2CNEt_2){\cdot}3H_2O$ (0.01 mol) and $AgNO_3$ (0.01 mol) were first dissolved in 50 mL of distilled water, respectively. Then, the two solutions were mixed with stirring in a 250 mL beaker for 2 h. And the resulting precipitates were collected by centrifugation (5000 rpm, 5 min) and washed several times with distilled water, and dried under a vacuum at 60 °C. $Zn(S_2CNEt_2)_2$, $In(S_2CNEt_2)_3$, $Fe(S_2CNEt_2)_3$ were synthesized by the same way as described above, except that the molar ratios of Zinc Chloride, Indium Chloride, Iron(III) Nitrate to $Na(S_2CNEt_2){\cdot}3H_2O$ were 1 to 2, 1 to 3, 1 to 3, respectively.

Synthesis of Ag_2S, Ag_2Se, and Ag_2Te Nanocrystals. In a typical procedure for Ag_2S, ODA (1.35 g) and 1.6 mL OA, 3.2 mL ODE were added in a 25 mL three-necked flask. Then, $Ag(S_2CNEt_2)$ (0.1 mmol) was added to the solution. The mixture was degassed and heated to 200 °C under nitrogen and kept for 30 min. The products were collected by centrifugation (8000 rpm, 5 min) and washed several times with *n*-hexane and absolute ethanol. All products in this paper were collected and washed by the same method. As for Ag_2Se, 5 mL OLA was added in a 25 mL three-necked flask. The solvent was heated to 180 °C under nitrogen, 0.2 g $AgNO_3$ was added to the solvent, the mixture was magnetically stirred for 10 min, and 0.048 g Se Powder was added to the mixture for a magnetically stirring of 30 min. As for Ag_2Te, ODA (1.35 g) and 1.6 mL OA, 3.2 mL ODE were added in a 25 mL three-necked flask. Then, 2 mL of 1 M TOP-Te was added to the solution. The mixture was degassed and heated to 190 °C under nitrogen, 0.17 g $AgNO_3$ was added to the mixture, and the mixture grew for 10 min at 150 °C.

Chemical Transformation of Ag_2S, Ag_2Se, and Ag_2Te Nanocrystals. In a typical procedure for Ag_2S, TPP (0.1 g) and the previous prepared Ag_2S nanocrystals were dispersed in 5 mL OLA in a 25 mL three-necked flask. The mixture was heated at 90 °C under vacuum for 20 min and then heated to 220 °C under nitrogen and kept for 10 min. As for Ag_2Se, one-fifth of the above obtained Ag_2Se nanocrystals, TOP (0.1 mL), and 5 mL OLA were added in a 25 mL three-necked flask. The mixture was heated at 90 °C under vacuum for 20 min and then heated to 220 °C under nitrogen and kept at for 10 min. As for Ag_2Te, the solution was heated to 250 °C under nitrogen and kept for 1 h.

Synthesis of Ag-Ni_3S_2 Heteronanostructures. In a typical procedure, $Ni(acac)_2$ (0.019 g), TPP (0.1 g), and the previous prepared Ag_2S nanocrystals were dispersed in 5 mL OLA in a 25 mL three-necked flask. The mixture was heated at 90 °C under vacuum for 20 min and then heated to 220 °C under nitrogen and kept for 30 min.

Synthesis of Ag_2S-ZnS Heteronanostructures. In a typical procedure, the above obtained Ag_2S, $Zn(S_2CNEt_2)_2$ (0.018 g), and 5 mL OLA were added in a 25 mL three-necked flask. The mixture was heated at 80 °C under vacuum for 20 min and then heated to 150 °C under nitrogen and kept for 30 min.

Chemical Transformation of Ag_2S-ZnS to Ag-ZnS Heteronanostructures. In a typical procedure, TPP (0.1 g) and the previous prepared Ag_2S-ZnS heteronanostructures were dispersed in 5 mL OLA in a 25 mL three-necked flask. The mixture was heated at 90 °C under vacuum for 20 min and then heated to 220 °C under nitrogen and kept for 30 min.

Synthesis of $AgFeS_2$ Nanocrystals. In a typical procedure, $AgNO_3$ (0.017 g), $Fe(S_2CNEt_2)_3$ (0.025 g), and 5 mL OLA were added in a 25 mL three-necked flask. The mixture was degassed and heated to 150 °C under nitrogen and kept for 30 min.

Chemical Transformation of $AgFeS_2$ to Ag Nanostructures. In a typical procedure, the above obtained $AgFeS_2$, TPP (0.1 g) and 5 mL OLA were added in a 25 mL three-necked flask. The mixture was heated at 90 °C under vacuum for 20 min and then heated to 220 °C under nitrogen and kept for 10 min.

Synthesis of $AgInS_2$ Nanocrystals. In a typical procedure, $Ag(S_2CNEt_2)$ (0.013 g), $In(S_2CNEt_2)_3$ (0.028 g), 5 mL OA, and 11

DOI: 10.1021/jacs.5b00041
J. Am. Chem. Soc. 2015, 137, 5390−5396

mL DDT were added in a 25 mL three-necked flask. The mixture was heated at 80 °C under vacuum for 20 min and then heated to 200 °C under nitrogen and kept for 2 h.

Chemical Transformation of $AgInS_2$ to Ag-$AgInS_2$ or Ag Heteronanostructures. In a typical procedure, TOP (0.2 mL) and the previous prepared $AgInS_2$ nanocrystals were dispersed in 5 mL OLA in a 25 mL three-necked flask. The mixture was heated at 90 °C under vacuum for 20 min and then heated to 250 °C under nitrogen and kept for 1 h. As for complete transformation, the reaction was kept at 250 °C for 10h using 1 mL TOP instead.

Synthesis of Bi_2S_3 Nanorods. In a typical procedure, $BiCl_3$ (0.5 g) and 10 mL OLA were added in a 25 mL three-necked flask. The mixture was heated at 120 °C under vacuum for 30 min and then heated to 170 °C under nitrogen and kept for 30 min. Then, 0.25 g S powder in 5 mL OLA was injected to the mixture and the mixture grew for 1 h at 130 °C.

Chemical Transformation of Bi_2S_3 Nanorods to Bi Nanocrystals. In a typical procedure, one-tenth of the above obtained Bi_2S_3, TPP (0.1 g), and 5 mL OLA were added in a 25 mL three-necked flask. The mixture was heated at 90 °C under vacuum for 20 min. Then, the mixture was heated under nitrogen to 220 °C and kept for 2 h.

Synthesis of $AgBiSe_2$ Nanocrystals. In a typical procedure, $BiCl_3$ (0.0788 g) and 10 mL OLA were added in a 25 mL three-necked flask. The mixture was heated under vacuum at 120 °C for 30 min. Then, the mixture was heated under nitrogen to 180 °C, and 0.0425 g $AgNO_3$ was added to the mixture. After magnetically stirring for 10 min, 0.040 g Se powder was added, and the mixture was kept at 180 °C for 30 min under magnetic stirring.

Chemical Transformation of $AgBiSe_2$ to Ag-Bi Core−Shell Nanostructures. In a typical procedure, TOP (0.2 mL) and half of the above prepared $AgBiSe_2$ nanocrystals were dispersed in 5 mL OLA in a 25 mL three-necked flask. The mixture was heated at 90 °C under vacuum for 20 min. Then, the mixture was heated to 220 °C under nitrogen and kept for 1 h.

Synthesis of Cu_3BiS_3 Nanocrystals. In a typical procedure, 2.25 mmol $Cu(acac)_2$, 0.75 mmol $Bi(NO_3)_3{\cdot}5H_2O$, and 12 mL OLA were added in a 25 mL three-necked flask. The mixture was heated at 140 °C under vacuum for 1 h. Then, the mixture was heated to 220 °C under nitrogen and 2.5 mL 1.2 M of S-OLA was injected, and the mixture was kept at 220 °C for 30 min under magnetic stirred.

Chemical Transformation of Cu_3BiS_3 to Bi-Cu_7S_4 Heteronanostructures. In a typical procedure, TPP (0.1 g) and one-fifth of the previous prepared Cu_3BiS_3 nanocrystals were dispersed in 5 mL OLA in a 25 mL three-necked flask. The mixture was heated at 90 °C under vacuum for 20 min and then heated to 220 °C under nitrogen and kept for 10 min.

Characterization. The product was characterized by XRD, using a Philips X'Pert PRO SUPER X-ray diffractometer equipped with graphite monochromaticized Cu Karadiation (λ = 1.54056 Å). The operation voltage and current were kept at 40 kV and 400 mA, respectively. TEM and HRTEM were performed on Hitachi H-7650 and JEOL-F2010 with an acceleration voltage of 200 kV respectively. STEM EDS element mapping and line scan were carried out on Inca Oxford equipped on JEOL-F2010.

■ ASSOCIATED CONTENT

Ⓢ Supporting Information

Additional XRD, TEM, and HRTEM analysis. This material is available free of charge via the Internet at http://pubs.acs.org.

■ AUTHOR INFORMATION

Corresponding Author

*shyu@ustc.edu.cn

Author Contributions

§The authors contributed equally.

Notes

The authors declare no competing financial interest.

■ ACKNOWLEDGMENTS

This work is supported by the Ministry of Science and Technology of China (Grants 2014CB931800, 2013CB933900), the National Natural Science Foundation of China (Grants 21431006, 91022032), the Chinese Academy of Sciences (Grant KJZD-EW-M01-1), and the China Postdoctoral Science Foundation (2013M540522).

■ REFERENCES

(1) Peng, X. G. *Acc. Chem. Res.* **2010**, *43*, 1387−1395.
(2) Burda, C.; Chen, X. B.; Narayanan, R.; El-Sayed, M. A. *Chem. Rev.* **2005**, *105*, 1025−1102.
(3) Cortie, M. B.; McDonagh, A. M. *Chem. Rev.* **2011**, *111*, 3713−3735.
(4) Zhuang, Z.; Peng, Q.; Li, Y. *Chem. Soc. Rev.* **2011**, *40*, 5492−5513.
(5) Schaak, R. E.; Mallouk, T. E. *Chem. Mater.* **2002**, *14*, 1455−1471.
(6) Costi, R.; Saunders, A. E.; Banin, U. *Angew. Chem., Int. Ed.* **2010**, *49*, 4878−4897.
(7) Cozzoli, P. D.; Pellegrino, T.; Manna, L. *Chem. Soc. Rev.* **2006**, *35*, 1195−1208.
(8) de Mello Donega, C. *Chem. Soc. Rev.* **2011**, *40*, 1512−1546.
(9) Buck, M. R.; Bondi, J. F.; Schaak, R. E. *Nat. Chem.* **2012**, *4*, 37−44.
(10) Yin, Y.; Alivisatos, A. P. *Nature* **2005**, *437*, 664−670.
(11) Kovalenko, M. V.; Scheele, M.; Talapin, D. V. *Science* **2009**, *324*, 1417−1420.
(12) Milliron, D. J.; Hughes, S. M.; Cui, Y.; Manna, L.; Li, J.; Wang, L. W.; Alivisatos, A. P. *Nature* **2004**, *430*, 190−195.
(13) Zhou, Y. L.; Yang, M.; Sun, K.; Tang, Z. Y.; Kotov, N. A. *J. Am. Chem. Soc.* **2010**, *132*, 6006−6013.
(14) Xia, Y. S.; Nguyen, T. D.; Yang, M.; Lee, B.; Santos, A.; Podsiadlo, P.; Tang, Z. Y.; Glotzer, S. C.; Kotov, N. A. *Nat. Nanotechnol.* **2011**, *6*, 580−587.
(15) Buonsanti, R.; Grillo, V.; Carlino, E.; Giannini, C.; Gozzo, F.; Garcia-Hernandez, M.; Garcia, M. A.; Cingolani, R.; Cozzoli, P. D. *J. Am. Chem. Soc.* **2010**, *132*, 2437−2464.
(16) Casavola, M.; Grillo, V.; Carlino, E.; Giannini, C.; Gozzo, F.; Pinel, E. F.; Garcia, M. A.; Manna, L.; Cingolani, R.; Cozzoli, P. D. *Nano Lett.* **2007**, *7*, 1386−1395.
(17) Carbonea, L.; Cozzoli, P. D. *Nano Today* **2010**, *5*, 449−493.
(18) Chen, X. B.; Li, C.; Gratzel, M.; Kostecki, R.; Mao, S. S. *Chem. Soc. Rev.* **2012**, *41*, 7909−7937.
(19) Freeman, R.; Willner, I. *Chem. Soc. Rev.* **2012**, *41*, 4067−4085.
(20) Hochbaum, A. I.; Yang, P. D. *Chem. Rev.* **2010**, *110*, 527−546.
(21) Talapin, D. V.; Lee, J. S.; Kovalenko, M. V.; Shevchenko, E. V. *Chem. Rev.* **2010**, *110*, 389−458.
(22) Tang, J.; Kemp, K.; Hoogland, S.; Jeong, K.; Liu, H.; Levina, L.; Furukawa, M.; Wang, X.; Debnath, R.; Cha, D.; Chou, K.; Fischer, A.; Amassian, A.; Asbury, J.; Sargent, E. H. *Nat. Mater.* **2011**, *10*, 765−771.
(23) Wang, X.; Koleilat, G. I.; Tang, J.; Liu, H.; Kramer, I. J.; Debnath, R.; Brzozowski, L.; Barkhouse, D. A. R.; Levina, L.; Hoogland, S.; Sargent, E. H. *Nat. Photonics* **2011**, *5*, 480−484.
(24) Zhang, H.; Wang, H.; Xu, Y.; Zhuo, S.; Yu, Y.; Zhang, B. *Angew. Chem., Int. Ed.* **2012**, *51*, 1459−1463.
(25) Miszta, K.; Dorfs, D.; Genovese, A.; Kim, M. R.; Manna, L. *ACS Nano* **2011**, *5*, 7176−7183.
(26) Rivest, J. B.; Jain, P. K. *Chem. Soc. Rev.* **2013**, *42*, 89−96.
(27) Jain, P. K.; Amirav, L.; Aloni, S.; Alivisatos, A. P. *J. Am. Chem. Soc.* **2010**, *132*, 9997−9999.
(28) Luther, J. M.; Zheng, H. M.; Sadtler, B.; Alivisatos, A. P. *J. Am. Chem. Soc.* **2009**, *131*, 16851−16857.
(29) Saruyama, M.; So, Y.; Kimoto, K.; Taguchi, S.; Kanemitsu, Y.; Teranishi, T. *J. Am. Chem. Soc.* **2011**, *133*, 17598−17601.
(30) Deka, S.; Miszta, K.; Dorfs, D.; Genovese, A.; Bertoni, G.; Manna, L. *Nano Lett.* **2010**, *10*, 3770−3776.

DOI: 10.1021/jacs.5b00041
J. Am. Chem. Soc. 2015, 137, 5390−5396

(31) Li, H. B.; Zanella, M.; Genovese, A.; Povia, M.; Falqui, A.; Giannini, C.; Manna, L. *Nano Lett.* **2011**, *11*, 4964−4970.
(32) Robinson, R. D.; Sadtler, B.; Demchenko, D. O.; Erdonmez, C. K.; Wang, L. W.; Alivisatos, A. P. *Science* **2007**, *317*, 355−358.
(33) Son, D. H.; Hughes, S. M.; Yin, Y. D.; Alivisatos, A. P. *Science* **2004**, *306*, 1009−1012.
(34) Sadtler, B.; Demchenko, Denis O.; Zheng, H.; Hughes, S. M.; Merkle, M. G.; Dahmen, U.; Wang, L. W.; Alivisatos, A. P. *J. Am. Chem. Soc.* **2009**, *131*, 5285−5293.
(35) Yin, Y. D.; Rioux, R. M.; Erdonmez, C. K.; Hughes, S.; Somorjai, G. A.; Alivisatos, A. P. *Science* **2004**, *304*, 711−714.
(36) Hong, J. F.; Mato, K.; Roland, S.; Kornelius, N.; Eckhard, P.; Dietrich, H.; Margit, Z.; Ulrich, G. *Nat. Mater.* **2006**, *5*, 627−631.
(37) Henkes, A. E.; Vasquez, Y.; Schaak, R. E. *J. Am. Chem. Soc.* **2007**, *129*, 1896−1897.
(38) Gao, M. R.; Xu, Y. F.; Jiang, J.; Yu, S. H. *Chem. Soc. Rev.* **2013**, *42*, 2986−3017.
(39) Tang, Z. Y.; Wang, Y.; Shanbhag, S.; Kotov, N. A. *J. Am. Chem. Soc.* **2006**, *128*, 7036−7042.
(40) Tang, Z. Y.; Wang, Y.; Sun, K.; Kotov, N. A. *Adv. Mater.* **2005**, *17*, 358−363.
(41) Tang, Z. Y.; Wang, Y.; Shanbhag, S.; Giersig, M.; Kotov, N. A. *J. Am. Chem. Soc.* **2006**, *128*, 6730−6736.
(42) Casavola, M.; Buonsanti, R.; Caputo, G.; Cozzoli, P. D. *Eur. J. Inorg. Chem.* **2008**, 837−854.
(43) Mokari, T.; Aharoni, A.; Popov, I.; Banin, U. *Angew. Chem., Int. Ed.* **2006**, *45*, 8001−8005.
(44) Han, S. K.; Gu, C.; Gong, M.; Wang, Z. M.; Yu, S. H. *Small* **2013**, *9*, 3765−3769.
(45) Beberwyck, B. J.; Alivisatos, A. P. *J. Am. Chem. Soc.* **2012**, *134*, 19977−19980.
(46) Sines, I.; Schaak, R. E. *J. Am. Chem. Soc.* **2011**, *133*, 1294−1297.
(47) Du, Y. P.; Xu, B.; Fu, T.; Cai, M.; Li, F.; Zhang, Y.; Wang, Q. B. *J. Am. Chem. Soc.* **2010**, *132*, 1470−1471.
(48) Wang, D. S.; Xie, T.; Peng, Q.; Li, Y. D. *J. Am. Chem. Soc.* **2008**, *130*, 4016−4022.
(49) Zhu, G. X.; Xu, Z. *J. Am. Chem. Soc.* **2011**, *133*, 148−157.
(50) Deng, M.; Shen, S.; Wang, X.; Zhang, Y.; Xu, H.; Zhang, T.; Wang, Q. *CrystEngComm* **2013**, *15*, 6443−6447.
(51) Xiao, C.; Qin, X.; Zhang, J.; An, R.; Xu, J.; Li, K.; Cao, B.; Yang, J.; Ye, B.; Xie, Y. *J. Am. Chem. Soc.* **2012**, *134*, 18460−18466.
(52) Malakooti, R.; Cademartiri, L.; Akçakir, Y.; Petrov, S.; Migliori, A.; Ozin, G. A. *Adv. Mater.* **2006**, *18*, 2189−2194.
(53) Yan, C.; Gu, E.; Liu, F.; Lai, Y.; Li, J.; Liu, Y. *Nanoscale* **2013**, *5*, 1789−1792.
(54) Barrelet, C. J.; Wu, Y.; Bell, D. C.; Lieber, C. M. *J. Am. Chem. Soc.* **2003**, *125*, 11498−11499.
(55) Murray, C. B.; Norris, D. J.; Bawendi, M. G. *J. Am. Chem. Soc.* **1993**, *115*, 8706−8715.
(56) Peng, Z. A.; Peng, X. G. *J. Am. Chem. Soc.* **2002**, *124*, 3343−3353.

DOI: 10.1021/jacs.5b00041
J. Am. Chem. Soc. 2015, 137, 5390−5396